# Four-Center Six-Electron Interaction versus Lone Pair−Lone Pair Interaction between Selenium Atoms in Naphthalene Peri Positions

Warô Nakanishi,*,† Satoko Hayashi,† and Shinji Toyota‡

*Department of Material Science and Chemistry, Faculty of Systems Engineering, Wakayama University, 930 Sakaedani, Wakayama 640-8510, Japan, and Department of Chemistry, Faculty of Science, Okayama University of Science, 1-1 Ridaicho, Okayama 700-0005, Japan*

*Received May 8, 1998*

The X-ray crystallographic analysis of bis[8-(phenylselanyl)naphthyl]-1,1′-diselenide (**1**) and 1-(methylselanyl)-8-(phenylselanyl)naphthalene (**2**) showed that the four selenium atoms in **1** aligned linearly, while the Se−C(Me) and Se−C(Ph) bond in **2** declined by about 50° and 40° from the naphthyl plane, respectively. Ab initio molecular orbital calculations were performed on the models of **1** and **2**, model **a** ($H_bH_c{}^2Se\cdots H_a{}^1Se^3SeH_a\cdots{}^4SeH_bH_c$) and model **b** ($H_aH_b{}^1Se\cdots{}^2SeH_{a'}H_{b'}$), respectively, with the 6-311++G(3df,2pd) basis sets at the HF and MP2 levels, and the calculations reproduced well the observed structures and revealed the nature of the bonds constructed by the selenium atoms containing nonbonded interactions. The bond with four linearly aligned selenium atoms in model **a** can be analyzed with the 4c-6e model constructed with the nonbonded interaction between the two p-type lone pairs on the outside selenium atoms and the $\sigma^*$(Se−Se) orbital of the inside Se−Se bond, which results in charge transfer from the outside Se atoms to the inside Se atoms. The nonbonded interaction between the two p-type lone pairs at the Se atoms in model **b** is analyzed as a $\pi$-type 2c-4e bond. The bent structure in $H_b$-$^1Se\cdots{}^2Se-H_{b'}$ was demonstrated to be the result of the requirement to avoid the severe exchange repulsion between the filled p-type lone pairs at the two selenium atoms. The calculations on the other models, PhSeH···HSeSeH···HSePh and PhSeH···HSeMe, with the 6-311+G(d,p) basis sets at the DFT (B3LYP) level showed that the $\pi$-orbitals of the phenyl groups of the former interacted effectively with the 4c-6e orbitals but the $\pi$-orbitals of the latter did little with the 2c-4e orbitals due to the orthogonality of the two systems.

## Introduction

Lone pairs of heteroatoms bound to $\pi$-systems will interact with them if the orientation of the two orbitals is suitable for the interaction.[1] The lone pairs of heteroatoms often encounter such orbitals that may interact with the lone pairs, extending over the electron deficient atoms or groups in cationic species, partially positive centers of polar bonds, and radical centers, together with low-lying antibonding orbitals.[2] The interaction of the lone pairs occurs not only by the through-bond mechanism but also by the through-space mechanism in such cases. The naphthalene peri positions supply a suitable system for the lone pairs to interact by the through-space mechanism, which is of current interest.[3−6] The lone pair−lone pair interactions have been demonstrated to play an important role in the nonbonded spin−spin couplings between fluorine−fluorine,[7] fluorine−nitrogen,[8] fluorine−selenium,[6d] and selenium−selenium.[4,6c,9]

Lone pairs of chalcogens have been represented by two types of orbitals; the one is depicted by the two $sp^3$-hybrid orbitals as shown in **A**, and the other is based on the p-

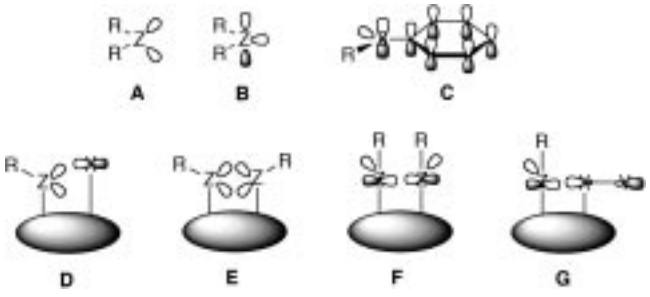


and s-type orbitals or p- and $sp^2$-hybrid orbitals as shown in **B**.[5] The $sp^3$-hybrid orbital model is convenient when one discusses the collective properties of chalcogenides such as the electron densities or the total energies of lone

† Wakayama University.
‡ Okayama University of Science.

(1) Topson, R. D. The Nature and Analysis of Substituent Electronic Effects. In *Progress in Physical Organic Chemistry*; Taft, R. W., Ed.; John Wiley & Sons: New York, 1976; Vol. 12. See also references cited therein.

(2) Bernardi, F., Csizmadia, I. G., Mangini, A., Eds. *Organic Sulfur Chemistry: Theoretical and Experimental Advances*; Elsevier Scientific: Amsterdam, 1985 and references therein.

(3) (a) Asmus, K.-D. *Acc. Chem. Res.* **1979**, *12*, 436. Musker, W. K. *Acc. Chem. Res.* **1980**, *13*, 200. (b) Fujihara, H.; Furukawa, N. *J. Mol. Struct.: THEOCHEM* **1989**, *186*, 261.

(4) (a) Fujihara, H.; Ishitani, H.; Takaguchi, Y.; Furukawa, N. *Chem. Lett.* **1995**, 571. (b) Fujihara, H.; Yabe, M.; Chiu, J.-J.; Furukawa, N. *Tetrahedron Lett.* **1991**, *32*, 4345. Furukawa, N.; Fujii, T.; Kimura, T.; Fujihara, H. *Chem. Lett.* **1994**, 1007. (c) Fujihara, H.; Saito, R.; Yabe, M.; Furukawa, N. *Chem. Lett.* **1992**, 1437.

(5) (a) Glass, R. S.; Andruski, S. W.; Broeker, J. L. *Rev. Heteroat. Chem.* **1988**, *1*, 31. (b) Glass, R. S.; Andruski, S. W.; Broeker, J. L.; Firouzabadi, H.; Steffen, L. K.; Wilson, G. S. *J. Am. Chem. Soc.* **1989**, *111*, 4036. (c) Glass, R. S.; Adamowicz, L.; Broeker, J. L. *J. Am. Chem. Soc.* **1991**, *113*, 1065.

(6) (a) Nakanishi, W. *Chem. Lett.* **1993**, 2121. (b) Nakanishi, W.; Hayashi, S.; Toyota, S. *J. Chem. Soc., Chem. Commun.* **1996**, 371. (c) Nakanishi, W.; Hayashi, S.; Yamaguchi, H. *Chem. Lett.* **1996**, 947. (d) Nakanishi, W.; Hayashi, S.; Sakaue, A.; Ono, G.; Kawada, Y. *J. Am. Chem. Soc.* **1998**, *120*, 3635.

10.1021/jo980885l CCC: $15.00 
Published on Web 11/03/1998

pairs. The p- and s-type orbitals must be employed if the one-electron properties such as the energy of each molecular orbital are discussed containing the lone pair orbital(s).[10] Since the p-type orbital of a lone pair has $C_s$ symmetry, it interacts with $\pi$-orbitals of aryl groups to which the lone pair orbital is attached if the orientation is suitable (**C**), as mentioned above. Lone pair orbitals interact with orbitals of other atoms or groups (**D**) and with other lone pairs (**E**), of which lone pairs are exemplified by $sp^3$-hybrid orbitals. The interaction between lone pairs will construct $\sigma$ bond(s) when two or more p-type orbitals of lone pairs align linearly (**F**), and the p-type orbitals are expected to interact with $\sigma$-bonds if the energy levels of the $\sigma^*$-orbitals are low enough for the interaction (**G**).

Parthasarathy et al. have suggested that there are two types of directional preferences of nonbonded atomic contacts with divalent chalcogens such as sulfur[11] and selenium,[12] R−Z−R′ (Z = S and Se). Type I contacts are with electrophiles, which have Z···X directions in RR′Z···X where n-electrons of sulfides or selenides are located (**D**), and type II contacts are with nucleophiles tending to lie along the extension of one of sulfur's or selenium's bond (**G** for X = S, Se). Electrophiles and nucleophiles should interact preferentially with the HOMO of the lone pair of Z and with the LUMO of the $\sigma^*$(Z−R) or $\sigma^*$(Z−R′) orbital, respectively. Glass and co-workers have shown that the lone pairs of sulfur atoms in naphtho[1,8-*b*,*c*]-1,5-dithiocin interact directly with each other, since the two orbitals lay on the naphthyl plane, while those in 1,8-bis(methylthio)naphthalene mainly interact with its $\pi$-system.[5] The former is an example of the interaction shown by **F**, and the latter is like that in **C**.

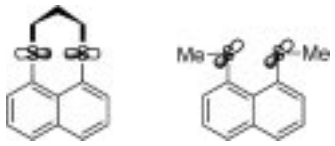


We have been interested in the intramolecular interaction in group 16 elements, especially that in selenium atoms.[6] We started our project to prepare such organoselenium compounds that are the typical examples of the lone pair−lone pair interactions shown in **D**−**G** and to examine the novel properties brought into the compounds by the interaction. Bis[8-(phenylselanyl)naphthyl]-1,1′-diselenide (**1**) and 1-(methylselanyl)-8-(phenylselanyl)naphthalene (**2**) were prepared as the first step of our investigations. The X-ray crystallographic analyses of **1** and **2** reveal that the four selenium atoms in **1** align linearly while the Se−C(Me) and Se−C(Ph) bonds in **2** decline by about 50° and 40° from the naphthyl plane, respectively. Ab initio MO calculations exhibit that the linear bond formed by the four selenium atoms in **1** can be analyzed by the four-center six-electron bond (4c-6e) model and the interaction between the lone pairs in **2** is characterized by the $\pi$-type two-center four-electron (2c-4e) interaction. We would like to present the results of the investigation of **1** and **2** based on the X-ray crystallographic analysis and ab initio MO calculations.

**Table 1. Selected Crystal Data and Structure Refinement for 1 and 2**

| | 1 | 2 |
|---|---|---|
| formula | $C_{32}H_{22}Se_4$ | $2 \times C_{17}H_{14}Se_2$ |
| fw, g mol$^{-1}$ | 722.37 | 2 × 376.22 |
| cryst syst | triclinic | triclinic |
| space group | P$\bar{1}$(no. 2) | P$\bar{1}$(no. 2) |
| color | yellow | colorless |
| *a*, Å | 12.2175(8) | 10.660(2) |
| *b*, Å | 12.3430(8) | 11.509(3) |
| *c*, Å | 9.7474(8) | 12.021(3) |
| α, ° | 103.038(6) | 90.40(2) |
| *β*, ° | 110.715(5) | 96.29(2) |
| *γ*, ° | 91.791(6) | 92.75(2) |
| *V*, Å$^3$ | 1329.5(2) | 1464.0(6) |
| $D_{calcd}$, g cm$^{-3}$ | 1.804 | 1.707 |
| *Z* | 2 | 4 |
| scan width, deg | 1.73 + 0.30 tan *θ* | 0.96 + 0.35 tan *θ* |
| $2\theta_{max}$, deg | 120.1 | 55.0 |
| no. of observations | 3669 | 3700 |
| no. of variables | 414 | 412 |
| *R* | 0.055 | 0.043 |
| $R_w$ | 0.065 | 0.050 |
| goodness-of-fit | 3.89 | 2.32 |

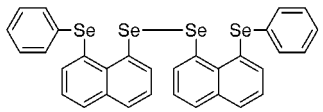


**1**

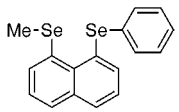


**2**

## Results and Discussion

**Structure of 1 and 2.** The reaction between the dianion of naphtho[1,8-*c*,*d*]-1,2-diselenol and 2 or more equiv of benzenediazonium ion at low temperature, followed by a usual workup, gave bis[8-(phenylselanyl)-naphthyl]-1,1′-diselenide (**1**).[6b] Reduction of **1** with sodium borohydride followed by the reaction with methyl iodide gave 1-(methylselanyl)-8-(phenylselanyl)naphthalene (**2**).[6c]

Single crystals of **1** and **2** were obtained via slow evaporation of hexane solutions, and each of the suitable crystals was subjected to X-ray crystallographic analysis. The crystallographic data are collected in Table 1. The selected interatomic distances, angles, and torsional angles of **1** and **2** are shown in Tables 2 and 3, respectively. Two independent molecules (structure **A** and structure **B**) were found in an asymmetric unit of the crystal of **2** (see Table 3). Figures 1 and 2 depict the structure of **1** and structure **A** of **2**, respectively.[13]

As shown in Figure 1, the two naphthyl planes in **1** are almost perpendicular with each other, which must

(7) (a) Mallory, F. B. *J. Am. Chem. Soc.* **1973**, *95*, 7747. (b) Mallory, F. B.; Mallory, C. W.; Fedarko, M.-C. *J. Am. Chem. Soc.* **1974**, *96*, 3536. (c) Mallory, F. B.; Mallory, C. W.; Ricker, W. M. *J. Am. Chem. Soc.* **1975**, *97*, 4770. Mallory, F. B.; Mallory, C. W.; Ricker, W. M. *J. Org. Chem.* **1985**, *50*, 457. Mallory, F. B.; Mallory, C. W.; Baker, M. B. *J. Am. Chem. Soc.* **1990**, *112*, 2577. (d) Ernst, L.; Ibrom, K. *Angew. Chem., Int. Ed. Engl.* **1995**, *34*, 1881. Ernst, L.; Ibrom, K.; Marat, K.; Mitchell, R. H.; Bodwell, G. J.; Bushnell, G. W. *Chem. Ber.* **1994**, *127*, 1119.

(8) Mallory, F. B.; Luzik, E. D., Jr. Mallory, C. W.; Carroll, P. J. *J. Org. Chem.* **1992**, *57*, 366. Mallory, F. B.; Mallory, C. W. *J. Am. Chem. Soc.* **1985**, *107*, 4816.

(9) Johannsen, I.; Eggert, H. *J. Am. Chem. Soc.* **1984**, *106*, 1240. Johannsen, I.; Eggert, H.; Gronowitz, S.; Hörnfeldt, A.-B. *Chem. Scr.* **1987**, *27*, 359. Fujihara, H.; Mima, H.; Erata, T.; Furukawa, N. *J. Am. Chem. Soc.* **1992**, *114*, 3117.

(10) Albright, T. A.; Burdett, J. K.; Whangbo, M.-H. *Orbital Interactions in Chemistry*; Wiley-Interscience: New York, 1985.

(11) Rosenfield, R. E., Jr.; Parthasarathy, R.; Dunitz, J. D. *J. Am. Chem. Soc.* **1977**, *99*, 4860.

(12) Ramasubbu, N.; Parthasarathy, R. *Phosphorus Sulfur* **1987**, *31*, 221.

(13) Although the discussion is focused on structure **A**, it is also valid on structure **B**.

**Table 2. Selected Interatomic Distances, Angles, and Torsional Angles of 1**

| | | | |
|---|---|---|---|
| **Interatomic Distances, Å** | | | |
| Se(1)−Se(2) | 3.018(1) | Se(1)−Se(3) | 2.365(1) |
| Se(3)−Se(4) | 3.087(1) | Se(1)−C(1) | 1.957(9) |
| Se(2)−C(9) | 1.915(9) | Se(3)−C(17) | 1.959(8) |
| Se(4)−C(25) | 1.909(9) | C(1)−C(10) | 1.42(1) |
| C(9)−C(10) | 1.41(1) | C(17)−C(26) | 1.42(1) |
| C(25)−C(26) | 1.42(1) | | |
| **Angles, deg** | | | |
| Se(2)−Se(1)−Se(3) | 177.10(5) | Se(1)−Se(3)−Se(4) | 170.45(5) |
| Se(3)−Se(1)−C(1) | 101.8(3) | Se(1)−Se(3)−C(17) | 103.1(3) |
| Se(1)−C(1)−C(10) | 122.6(7) | C(1)−C(10)−C(9) | 126.0(8) |
| Se(2)−C(9)−C(10) | 123.2(6) | C(9)−Se(2)−C(11) | 99.7(4) |
| Se(3)−C(17)−C(26) | 122.8(6) | C(17)−C(26)−C(25) | 127.5(8) |
| Se(4)−C(25)−C(26) | 124.7(6) | C(25)−Se(4)−C(27) | 100.6(4) |
| **Torsional Angles, deg** | | | |
| Se(2)−Se(1)−Se(3)−Se(4) | 157.3(8) | Se(1)−C(1)−C(10)−C(9) | 10(1) |
| C(1)−Se(1)−Se(3)−C(17) | 91.4(4) | Se(3)−Se(1)−C(1)−C(10) | 163.0(7) |
| Se(2)−C(9)−C(10)−C(1) | 12(1) | C(10)−C(9)−Se(2)−C(11) | 76.2(7) |
| Se(3)−C(17)−C(26)−C(25) | 6(1) | Se(1)−Se(3)−C(17)−C(26) | 179.0(7) |
| Se(4)−C(25)−C(26)−C(17) | 6(1) | C(26)−C(25)−Se(4)−C(27) | 70.0(8) |
| C(9)−Se(2)−C(11)−C(12) | 51.4(9) | C(25)−Se(4)−C(27)−C(28) | −162.0(7) |
| C(5)−C(10)−C(1)−C(2) | −7(1) | C(5) C(10)−C(9)−C(8) | 2(1) |

**Table 3. Selected Interatomic Distances, Angles, and Torsional Angles of 2**

| structure **A** | | structure **B** | |
|---|---|---|---|
| **Interatomic Distances, Å** | | | |
| Se(1A)−C(1A) | 1.931(8) | Se(1B)−C(1B) | 1.923(8) |
| Se(1A)−C(11A) | 1.936(9) | Se(1B)−C(11B) | 1.938(9) |
| Se(2A)−C(9A) | 1.937(8) | Se(2B)−C(9B) | 1.947(8) |
| Se(2A)−C(12A) | 1.933(8) | Se(2B)−C(12B) | 1.936(7) |
| Se(1A)−Se(2A) | 3.048(1) | Se(1B)−Se(2B) | 3.091(1) |
| C(1A)−C(10A) | 1.43(1) | C(1B)−C(10B) | 1.41(1) |
| C(9A)−C(10A) | 1.44(1) | C(9B)−C(10B) | 1.458(10) |
| **Angles, deg** | | | |
| C(1A)−Se(1A)−C(11A) | 97.8(4) | C(1B)−Se(1B)−C(11B) | 98.2(4) |
| Se(1A)−C(1A)−C(10A) | 122.9(6) | Se(1B)−C(1B)−C(10B) | 125.6(5) |
| C(9A)−Se(2A)−C(12A) | 98.4(3) | C(9B)−Se(2B)−C(12B) | 98.1(3) |
| Se(2A)−C(9A)−C(10A) | 123.1(6) | Se(2B)−C(9B)−C(10B) | 122.3(6) |
| C(1A)−C(10A)−C(9A) | 126.4(7) | C(1B)−C(10B)−C(9B) | 125.5(7) |
| Se(1A)−Se(2A)−C(12A) | 157.6(2) | Se(1B)−Se(2B)−C(12B) | 156.5(3) |
| Se(2A)−Se(1A)−C(11A) | 148.6(4) | Se(2B)−Se(1B)−C(11B) | 140.2(3) |
| **Torsional Angles, deg** | | | |
| C(11A)−Se(1A)−C(1A)−C(10A) | 133.0(7) | C(11B)−Se(1B)−C(1B)−C(10B) | −122.4(7) |
| Se(1A)−C(1A)−C(10A)−C(9A) | −10(1) | Se(1B)−C(1B)−C(10B)−C(9B) | 13(1) |
| C(2A)−C(1A)−Se(1A)−C(11A) | 43.1(7) | C(2B)−C(1B)−Se(1B)−C(11B) | −52.3(7) |
| C(12A)−Se(2A)−C(9A)−C(10A) | 143.2(6) | C(12B)−Se(2B)−C(9B)−C(10B) | −141.8(6) |
| Se(2A)−C(9A)−C(10A)−C(1A) | −8(1) | Se(2B)−C(9B)−C(10B)−C(1B) | 7(1) |
| C(9A)−Se(2A)−C(12A)−C(13A) | 87.7(7) | C(9B)−Se(2B)−C(12B)−C(13B) | 97.5(7) |
| C(9A)−Se(2A)−C(12A)−C(17A) | −97.8(7) | C(9B)−Se(2B)−C(12B)−C(17B) | −87.8(7) |
| C(8A)−C(9A)−Se(2A)−C(12A) | 31.3(7) | C(8B)−C(9B)−Se(2B)−C(12B) | −33.1(7) |
| C(11A)−Se(1A)−Se(2A)−C(12A) | 170.9(9) | C(11B)−Se(1B)−Se(2B)−C(12B) | −169.0(8) |
| C(5A)−C(10A)−C(1A)−C(2A) | 6(1) | C(5B)−C(10B)−C(1B)−C(2B) | −6(1) |
| C(5A)−C(10A)−C(9A)−C(8A) | −3(1) | C(5B)−C(10B)−C(9B)−C(8B) | 4(1) |

be a reflection of those in ArSeSeAr.[14] The planarity of the naphthyl planes was good; the torsional angles of C(5)C(10)C(1)C(2) and C(5)C(10)C(9)C(8) were −7(1)° and 2(1)°, respectively. The four selenium atoms in **1** lay almost on the planes; the torsional angles of Se(1)C(1)C(10)C(9), Se(2)C(9)C(10)C(1), Se(3)Se(1)C(1)C(10), Se(3)C(17)C(26)C(25), Se(4)C(25)C(26)C(17), and Se(1)Se(3)C(17)C(26) were 10(1)°, 12(1)°, 163.0(7)°, 6(1)°, 6(1)°, and 179.0(7)°, respectively. The C(1)Se(1)Se(3) and Se(1)Se(3)C(17) angles and the torsional angle C(1)Se(1)Se(3)C(17) around the diselenide moiety were 101.8(3)°, 103.1(3)°, and 91.4(4)°, respectively. The angles for Se(3)Se(1)Se(2) and Se(1)Se(3)Se(4) and the torsional angle for Se(2)Se(1)Se(3)Se(4) were 177.10(5)°, 170.45(5)°, and 157.3(8)°, respectively. Each phenyl group is located near the naphthyl group to which the phenyl group is not bonded (roof structure). The C(nap)−Se(Se) bonds of **1** may rotate freely, which results in the zigzag alignment for the four Se atoms of **1** (cf. Scheme 1d); however, the two C(nap)−Se(Se) bonds rotate for the naphthyl planes to be perpendicular with each other. The fact that the two naphthyl planes meet at about a right angle is also an important factor for the linear alignment of the four Se atoms, which must be a reflection of the torsional angles of two Se−C bonds in usual diaryl diselenides being about 90°.[14] The linear alignment of the four selenium atoms detected in **1** is the first observation of this to the best of our knowledge.

As shown in Figure 2, the planarity of the naphthyl planes of the bis-selenide **2** (structure **A**) was also good;

(14) Marsh, R. E. *Acta Crystallogr.* **1952**, *5*, 458. Kruse, F. H.; Marsh, R. E.; McCullough, J. D. *Acta Crystallogr.* **1957**, *10*, 201. Potrzebowski, M. J.; Michalska, M.; Blaszczyk, J.; Wieczorek, M. W.; Ciesielski, W.; Kazmierski, S.; Pluskowski, J. *J. Org. Chem.* **1995**, *60*, 3139.

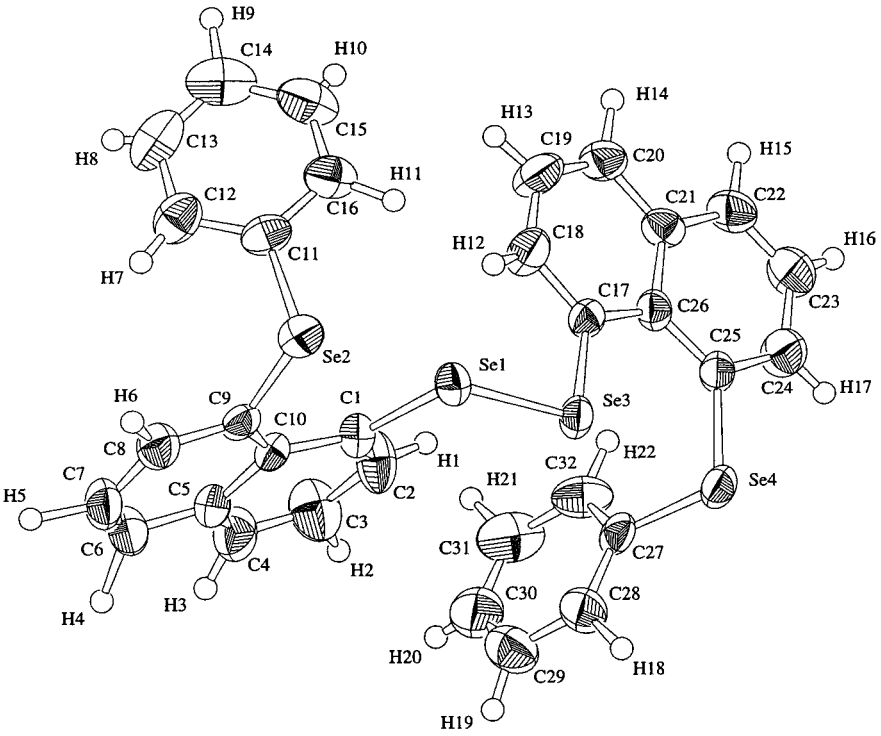


**Figure 1.** ORTEP drawing of **1**.

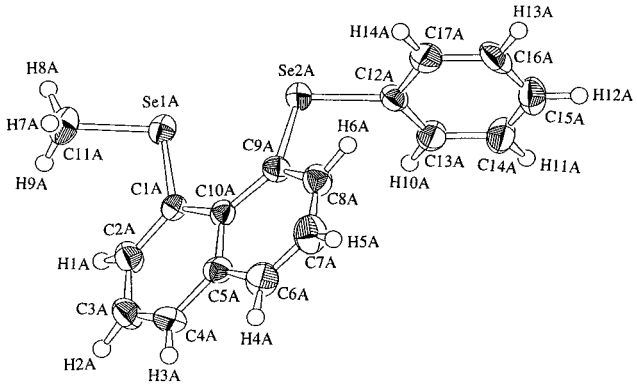


**Figure 2.** ORTEP drawing of **2** (structure **A**).

**Scheme 1**

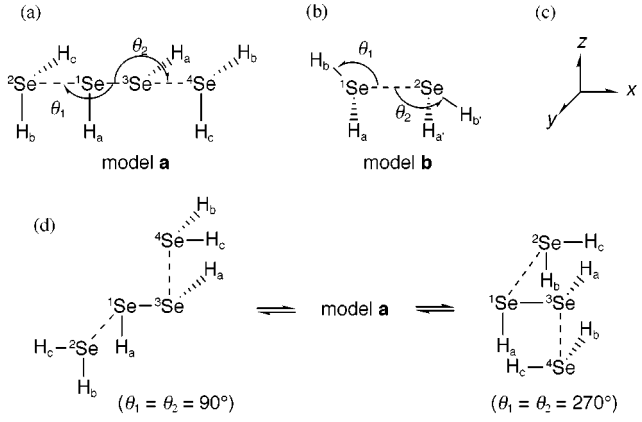


the torsional angles of C(5A)C(10A)C(1A)C(2A) and C(5A)C(10A)C(9A)C(8A) were 6(1)° and −3(1)°, respectively. The two selenium atoms slightly deviated from the plane; the torsional angles of Se(1A)C(1A)C(10A)C(9A) and Se(2A)C(9A)C(10A)C(1A) were −10(1)° and −8(1)°, respectively. The Se−C(Me) and Se−C(Ph) bonds of structure **A** and structure **B** in **2** decline by about 50° and 40° from the naphthyl plane, respectively; the torsional angles of C(11A)Se(1A)C(1A)C(10A) and C(12A)-Se(2A)C(9A)C(10A) of structure **A** were 133.0(7)° and 143.2(6)°, respectively, and those of C(11B)Se(1B)C(1B)C-(10B) and C(12B)Se(2B)C(9B)C(10B) of structure **B** were −122.4(7)° and −141.8(6)°, respectively.

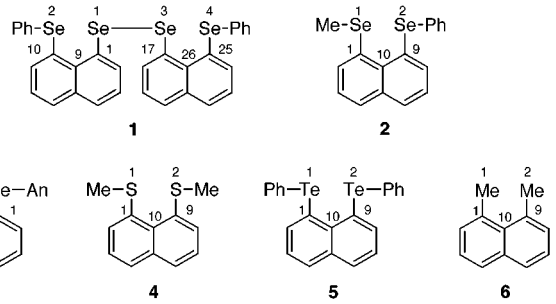


Table 4 collects the nonbonded distances between atoms at the peri positions and the selected angles and torsional angles of the naphthalenes, **1**−**6**.[4a,5c,6d,15] The nonbonded Se···Se distances in **1** were 3.018(1) and 3.087(1) Å for Se(1)···Se(2) and Se(3)···Se(4), respectively (3.053 Å on average). That for Se(1)···Se(2) in structure **A** of **2** was 3.048(1) Å, and the corresponding value for structure **B** was 3.091(1) Å, which is shown in Table 4 (3.070 Å on average). Since the sum of the van der Waals radii[16] of the two Se atoms is 4.00 Å, the nonbonded Se···Se distances in **1** and **2** are shorter than the van der Waals value by 0.95 and 0.93 Å, respectively ($\Delta r_v$(Se,Se) = 0.95 Å for **1** and 0.93 Å for **2**). The $\Delta r_v$(F,Se) in **3**,[6d] $\Delta r_v$(S,S) in **4**,[5c] $\Delta r_v$(Te,Te) in **5**,[4a] and $\Delta r_v$(C(Me),C(Me))

(15) Bright, D.; Maxwell, I. F.; de Boer, J. *J. Chem. Soc., Perkin Trans. 2* **1973**, 2101.
(16) Pauling, L. *The Nature of the Chemical Bond*, 3rd ed.; Cornell University Press: Ithaca, NY, 1960; Chapter 7. See also, Bondi, A. *J. Phys. Chem.* **1964**, *68*, 441.

**Table 4. Nonbonded Distances, Angles, and Torsional Angles of Some Peri-Substituted Naphthalenes**

| compd | *r*(Z1,Z2) (*r*(Z3,Z4) | ∠Z1C1C10 ∠Z3C17C26 | ∠Z2C9C10 ∠Z4C25C26 | ∠C1C10C9 ∠C17C26C25 | ∠Z1C1C10C9 ∠Z3C17C26C25 | ∠Z2C9C10C1 ∠Z4C25C26C17 | ∠C10C1Z1M ∠C26C17Z3M | ∠C10C9Z2C ∠C26C25Z4C) |
|---|---|---|---|---|---|---|---|---|
| **1** | 3.018(1) | 122.6(7) | 123.2(6) | 126.0(8) | 10(1) | 12(1) | −163.0(7) | 76.2(7) |
| | (3.087(1) | 122.8(6) | 124.7(6) | 127.5(8) | 6(1) | 6(1) | −179.0(7) | 70.0(8)) |
| **2**[a] | 3.048(1) | 122.9(6) | 123.1(6) | 126.4(7) | −10(1) | −8(1) | −133.0(7) | −143.2(6) |
| **2**[b] | 3.091(1) | 125.6(5) | 122.3(6) | 125.5(7) | 13(1) | 7(1) | 122.4(7) | 141.8(6) |
| **3**[c] | 2.753(3) | 120.5(3) | 119.1(3) | 125.9(3) | −0.1(5) | 1.2(6) | 179.2(3) | |
| **3**[d] | 2.744(3) | 120.7(3) | 118.7(4) | 125.6(4) | −0.9(6) | −3.7(6) | 162.8(3) | |
| **4**[e] | 2.918(2) | 122.5(3) | 121.1(3) | 126.3(4) | −8.3 | −8.9 | 143.2 | 158.3 |
| **4**[f] | 2.934(2) | 122.1(3) | 123.5(3) | 125.4(4) | −6.4 | −7.6 | 142.0 | 153.0 |
| **5** | 3.29 | 123(1) | 124(1) | 128(1) | −12.0 | −16.2 | *g* | *g* |
| **6** | 2.932 | 124.8(1) | 124.7(1) | 125.2(1) | −0.015 | 0.001 | | |

[a] For structure **A**. [b] For structure **B**. [c] For structure **A** in ref 1. [d] For structure **B** in ref 1. [e] For structure **1** in ref 5c. [f] For structure **2** in ref 5c. [g] Structure of type **C** for both the Te atoms being suggested in the figure, although the values were not specified.

in **6**[15] were 0.60, 0.77, 1.11, and 1.07 Å, respectively. The $\Delta r_v$ value becomes large as the sum of the van der Waals radii increase. The $\Delta r_v$ values must be strongly controlled by the intrinsic distance of the peri positions where the two atoms are bonded, the chalcogen−carbon bond distances, and their van der Waals values.

Three types of directional preferences are found around the divalent selenium atoms drawn in the perspective view of **1** and **2** (**7** and **8**, respectively). Such a view is also shown for **3** (**9**). The types can be classified by the perspective angle $\theta$ shown in **10**; we call the direction type A if $\theta$ is ca. 90° or less, type B when $\theta$ is ca. 180°, and type C when $\theta$ is ca. 135°. The structure of **1** exhibits type A for the two outside phenylselanyl groups and type B for the central Se−Se group. The methylselanyl and phenylselanyl groups in **2** belong to type C. The chalcogen atoms in the methylthio and phenyltelluro groups in **4** and **5** also belong to type C. The *p*-anisylselanyl group in **3** is one of the typical examples that belongs to type B.

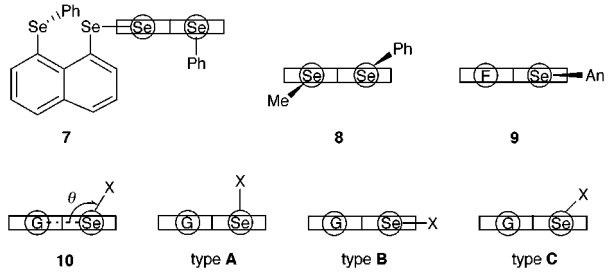


Parthasarathy et al. have suggested that there are two types of directional preferences of nonbonded atomic contacts with divalent sulfur, R−S−R′.[11] Type I contacts have S···X directions in RR′S···X where n-electrons of sulfides are located, and type II contacts tend to lie along the extension of one of sulfur's bond. Nearly all type I contacts are with electrophiles, while nearly all type II contacts are with nucleophiles. Electrophiles should interact preferentially with the HOMO and nucleophiles with the LUMO. The type I pattern suggests that the HOMO is essentially a sulfur lone pair extending nearly perpendicular to the R−S−R′ plane, while the type II pattern indicates the LUMO of a $\sigma^*$(S−R) or $\sigma^*$(S−R′) orbital. Similar directional preferences of nonbonded atomic contacts have also been seen with divalent selenium.[12] Type A and type B of our case belong to type I and type II of Parthasarathy's definitions, respectively, if one recognizes G in **10** to be the nucleophile or electrophile. Type C is the intermediate between type I and type II or the edge of the type II.

When two divalent selenium atoms are placed in close proximity in space, two types of pairings are suggested to play an important role among a lot of possibilities.[12] The one is the type I and type II pairing, and the other is type III, where the $\theta$ values of the paired selenides are almost equal.[17] The structure of **1** is recognized to consist of two sets of the type I and type II pairing with the linear alignment of the four selenium atoms. The type I and type II pairing must be stabilized by the electron donor−acceptor interaction. The p-type lone pairs at the two selenium atoms of the phenylselanyl groups must act as electron donors, while the $\sigma^*$(Se−Se) bond must accept the electrons from the phenylselanyl groups. Since the two 4p-type lone pairs and the $\sigma^*$(Se−Se) bonds of the 4p atomic orbitals in **1** interact linearly, the interaction should be analyzed by the 4c-6e model, of which the four electrons come from the two lone-pair orbitals and the two from the $\sigma$(Se−Se) bond. The structure of **2**, as well as those of **4** and **5**, belongs to the type III pairing. No special stabilizing factors can be found for the type III pairing in **2**,[12] at first glance. The steric or static repulsion of the selanyl groups may be reduced in the type III pairing. Ab initio MO calculations were performed to elucidate the nature of the 4c-6e bond in **1** and to clarify the stabilizing factors of the type III pairing in **2**.

**Molecular Orbital Calculations on the Model Compounds of 1 and 2.** Why is the linear alignment of the four selenium atoms more stable than the bent forms usually observed in polyselenides?[18] The effective interaction of the 4p-type lone-pair orbitals of the outside Se atoms with the 4p−4p $\sigma^*$ orbital of the Se(1)−Se(3) bond is suggested by the structure of **1**. The factor that stabilizes the structure of **2** is also interesting. Ab initio MO calculations were performed with the 6-311++G-(3df,2pd) basis sets of the Gaussian 94 program[19] on the models of **1** and **2** at the HF and MP2 levels. The simplified models, $H_bH_c{}^2Se\cdots H_a{}^1Se^3SeH_a\cdots{}^4SeH_bH_c$ (model

(17) Parthasarathy et al. defined $\theta$ from the normal to the selenide plane; see refs 11 and 12.

(18) (a) Takeda, N.; Tokitoh, N.; Imakubo, T.; Goto, M.; Okazaki, R. *Bull. Chem. Soc. Jpn.* **1995**, *68*, 2757. Tokitoh, N. *J. Synth. Org. Chem. Jpn.* **1994**, *52*, 136. (b) Klayman, D. L.; Günther, W. H. H. *Organic Selenium Compounds: Their Chemistry and Biology*; Wiley: New York, 1973; Chapter II.

(19) Frisch, M. J.; Trucks, G. W.; Schlegel, H. B.; Gill, P. M. W.; Johnson, B. G.; Robb, M. A.; Cheeseman, J. R.; Keith, T.; Petersson, G. A.; Montgomery, J. A.; Raghavachari, K.; Al-Laham, M. A.; Zakrzewski, V. G.; Ortiz, J. V.; Foresman, J. B.; Cioslowski, J.; Stefanov, B. B.; Nanayakkara, A.; Challacombe, M.; Peng, C. Y.; Ayala, P. Y.; Chen, W.; Wong, M. W.; Andres, J. L.; Replogle, E. S.; Gomperts, R.; Martin, R. L.; Fox, D. J.; Binkley, J. S.; Defrees, D. J.; Baker, J.; Stewart, J. P.; Head-Gordon, M.; Gonzalez, C.; Pople, J. A. *Gaussian 94*, revision D.4; Gaussian, Inc.: Pittsburgh, PA, 1995.

**Table 5. Results of the MO Calculations for $H_cH_b{}^2Se\cdots{}^1SeH_a{}^3SeH_a\cdots{}^4SeH_bH_c$ (Model a),[a] $SeH_2$, and $Se_2H_2$**

| | *E* (au) | *r*(Se,Se) (Å) | *r*(Se,$H_a$) (Å) | *r*(Se,$H_b$) (Å) | *r*(Se,$H_c$) (Å) | ∠SeSe$H_a$ (deg) | $\theta_1(=\theta_2)$ (deg) | ∠SeSe$H_c$ (deg) | ∠$H_b$Se$H_c$ (deg) | $Q_n(^1Se)$ | $Q_n(H_a)$ | $Q_n(^2Se)$ | $Q_n(H_b)$ | $Q_n(H_c)$ |
|---|---|---|---|---|---|---|---|---|---|---|---|---|---|---|
| | | | | | | HF/6−311++G(3df,2pd) | | | | | | | | |
| **11a**[b] | −9602.6928 | 2.4030 | 1.4525 | 1.4533 | 1.4523 | 90.00[c] | 181.40 | 90.00[c] | 93.17 | −0.0988 | 0.0392 | −0.0551 | 0.0557 | 0.0590 |
| Δ[d] | 0.0307 | 0.0496 | −0.0008 | 0.0003 | −0.0007 | 0.00[c] | | 0.00[c] | −0.05 | −0.0519 | −0.0077 | 0.0513 | 0.0025 | 0.0058 |
| **11b**[b] | −9602.6966 | 2.3774 | 1.4545 | 1.4538 | 1.4584 | 90.00[c] | 161.73 | 151.88 | 91.91 | −0.0606 | 0.0442 | −0.0887 | 0.0545 | 0.0506 |
| Δ[d] | 0.0269 | 0.0240 | 0.0012 | 0.0008 | 0.0054 | 0.00[c] | | | −1.31 | −0.0137 | −0.0027 | 0.0177 | 0.0013 | −0.0028 |
| **11b′**[b] | −9602.6936 | 2.3644 | 1.4544 | 1.4547 | 1.4572 | 90.00[c] | 180.00[c] | 180.00[c] | 90.00[c] | −0.0515 | 0.0453 | −0.1085 | 0.0542 | 0.0605 |
| Δ[d] | 0.0293 | 0.0110 | 0.0011 | 0.0005 | 0.0030 | 0.00[c] | | | 0.00[c] | −0.0046 | −0.0016 | −0.0034 | 0.0016 | 0.0079 |
| $Se_2H_2$[b] | −4800.7867 | 2.3534 | 1.4533 | | | 90.00[c] | | | | −0.0469 | 0.0469 | | | |
| $SeH_2$ | −2400.9684 | | | 1.4530 | 1.4530 | 0.00[c] | | | 93.22 | | | −0.1064 | 0.0532 | 0.0532 |
| $SeH_2$ | −2400.9681 | | | 1.4542 | 1.4542 | | | | 90.00[c] | | | −0.1051 | 0.0526 | 0.0526 |
| | | | | | | MP2/6−311++G(3df,2pd) | | | | | | | | |
| **11a**[b] | −9603.3758 | 2.3915 | 1.4637 | 1.4604 | 1.4596 | 96.59 | 178.68 | 90.00 | 91.20 | −0.0965 | 0.0373 | −0.0557 | 0.0551 | 0.0598 |
| Δ[d] | 0.0071 | 0.0607 | −0.0004 | 0.0013 | 0.0005 | 0.48 | | | −0.07 | −0.0504 | −0.0088 | 0.0515 | 0.0015 | 0.0062 |
| **11b**[b] | −9603.3771 | 2.3679 | 1.4654 | 1.4607 | 1.4656 | 96.00 | 161.14 | 144.08 | 90.23 | −0.0656 | 0.0419 | −0.0831 | 0.0546 | 0.0522 |
| Δ[d] | 0.0058 | 0.0371 | 0.0013 | 0.0016 | 0.0065 | −0.11 | | | −1.04 | −0.0195 | −0.0042 | 0.0241 | 0.0010 | −0.0014 |
| **11b′**[b] | −9603.3721 | 2.3710 | 1.4646 | 1.4609 | 1.4649 | 90.00[c] | 180.00[c] | 180.00[c] | 90.00[c] | −0.0536 | 0.0474 | −0.1109 | 0.0553 | 0.0619 |
| Δ[d] | 0.0088 | 0.0163 | 0.0025 | 0.0053 | 0.0053 | 0.00[c] | | | 0.00[c] | −0.0051 | −0.0011 | −0.0041 | 0.0019 | 0.0085 |
| $Se_2H_2$ | −4801.1059 | 2.3308 | 1.4640 | | | 96.11 | | | | −0.0461 | 0.0461 | | | |
| $Se_2H_2$[b] | −4801.1059 | 2.3308 | 1.4641 | | | 96.11 | | | | −0.0461 | 0.0461 | | | |
| $Se_2H_2$[b] | −4801.1041 | 2.3547 | 1.4621 | | | 90.00[c] | | | | −0.0485 | 0.0485 | | | |
| $SeH_2$ | −2401.1385 | | | 1.4591 | 1.4591 | | | | 91.27 | | | −0.1072 | 0.0536 | 0.0536 |
| $SeH_2$ | −2401.1384 | | | 1.4596 | 1.4596 | | | | 90.00[c] | | | −0.1068 | 0.0534 | 0.0534 |

[a] *r*($^2$Se,$^1$Se) and *r*($^3$Se,$^4$Se) being fixed at 3.053 Å. [b] Torsional angle HSeSeH and ∠SeSeH of the $Se_2H_2$ moiety being fixed at 90.00°. [c] Fixed at the given value. [d] Values corresponding to the formation of the adduct from its components.

**Table 6. Natural Charges ($Q_n$) in $H_2{}^1Se\cdots{}^2SeH_2$ (Model b) and $SeH_2$ Calculated with the 6-311++G(3df,2pd) Basis Sets[a]**

| | level (au) | *E* (au) | *r*(Se,$H_a$) (Å) | *r*(Se,$H_b$) (Å) | $\theta_1$ (=$\theta_2$) (deg) | ∠$H_a$Se$H_b$ (deg) | $Q_n(^1Se)$ | $Q_n(H_a)$ | $Q_n(H_b)$ |
|---|---|---|---|---|---|---|---|---|---|
| **12a** | HF | −4801.9013 | 1.4521 | 1.4467 | 74.18 | 93.65 | −0.1000 | 0.0489 | 0.0511 |
| Δ | | 0.0355 | −0.0009 | −0.0063 | | 0.43 | 0.0064 | −0.0043 | −0.0021 |
| **12b** | HF | −4801.9222 | 1.4542 | 1.4587 | 158.95 | 91.64 | −0.0986 | 0.0511 | 0.0476 |
| Δ | | 0.0146 | 0.0012 | 0.0057 | | −1.58 | 0.0078 | −0.0021 | −0.0056 |
| $SeH_2$ | HF | −2400.9684 | 1.4530 | 1.4530 | | 93.22 | −0.1064 | 0.0532 | 0.0532 |
| **12a** | MP2 | −4802.2516 | 1.4589 | 1.4536 | 72.72 | 91.63 | −0.1012 | 0.0492 | 0.0520 |
| Δ | | 0.0254 | −0.0002 | −0.0055 | | 0.36 | 0.0060 | −0.0044 | −0.0016 |
| **12b** | MP2 | −4802.2714 | 1.4608 | 1.4665 | 157.43 | 89.77 | −0.0995 | 0.0522 | 0.0474 |
| Δ | | 0.0056 | 0.0017 | 0.0074 | | −1.50 | 0.0077 | −0.0014 | −0.0062 |
| $SeH_2$ | MP2 | −2401.1385 | 1.4591 | 1.4591 | | 91.27 | −0.1072 | 0.0536 | 0.0536 |

[a] The $C_2$ symmetry was postulated, and *r*($^2$Se,$^1$Se) was fixed at 3.070 Å.

**a**) and $H_aH_b{}^1Se\cdots{}^2SeH_{a'}H_{b'}$ (model **b**), are shown in Scheme 1. The rotation around the Se−$H_a$ bonds in model **a** would produce the zigzag alignment of the four selenium atoms; some possibilities are shown in Scheme 1d.

For model **a**, the two 1,8-naphthylidene groups in **1** are replaced by two sets of $H_a$ and $H_b$; the two $H_c$'s stand for phenyl groups. The atomic distances of *r*($^1$Se−$^2$Se) and *r*($^3$Se−$^4$Se) were fixed at the averaged value of the corresponding values observed in **1** (3.053 Å). The ∠$^1$Se$^2$Se$H_b$ and ∠$^3$Se$^4$Se$H_b$ values and the torsional angle of $H_a{}^1Se^3SeH_a$ were fixed at 90.00°. The torsional angles of $H_b{}^2Se^1SeH_a$ and $H_b{}^4Se^3SeH_a$ were fixed at 0.00°. While the ∠$^1$Se$^3$Se$H_a$ and ∠$^3$Se$^1$Se$H_a$ values were fixed at 90.00° for the calculations at the HF level, they were optimized at the MP2 level. Ab initio MO calculations were performed assuming the $C_2$ symmetry. The *r*($^1$Se−$^3$Se) and all *r*(Se−H) values were optimized. The angles $\theta_1$ (and $\theta_2$) and ∠$H_b{}^1SeH_c$ (and ∠$H_b{}^4SeH_c$) were also optimized. The calculations were carried out with or without fixing the torsional angles $H_aH_b{}^2SeH_c$ and $H_aH_b{}^4SeH_c$ at 90.00° and with them fixed at 180.00°. The results are given in Table 5 with the optimized structures shown by **11a**, **11b**, and **11b′**, respectively. Table 5 also contains the results of calculations for the corresponding structures of $H_2Se$ and $H_2Se_2$. Natural charges of the H and Se atoms of the model and the components were calculated with the natural population analysis.[20] The results are also shown in Table 5.

The optimized structures of model **a** at the MP2 level are as follows. $\theta_1$ (=$\theta_2$) was 178.68° (**11a**) when the

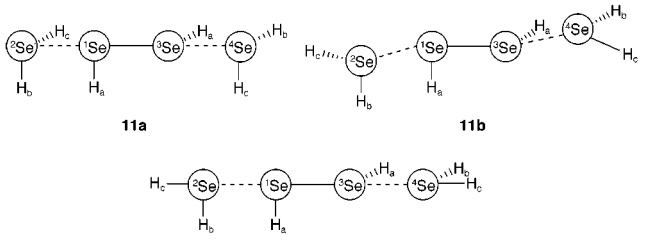


calculations were performed with the torsional angles $H_aH_b{}^2SeH_c$ and $H_aH_b{}^4SeH_c$ being fixed at 90.00°. Whereas $\theta_1$ (=$\theta_2$) and the torsional angles $H_aH_b{}^2SeH_c$ and $H_aH_b{}^4SeH_c$ were evaluated to be 161.14° and 144.08°, respectively, if the torsional angles were not fixed (**11b**). The MO calculations were also carried out on model **a** with $\theta_1$ (=$\theta_2$) and the torsional angle $H_aH_b{}^2SeH_c$ (and $H_aH_b{}^4SeH_c$) being fixed at 180.00° (**11b′**).

The 1,8-naphthylidene group in **2** is replaced by $H_a$ and $H_{a'}$ and the methyl and phenyl groups are by $H_b$ and $H_{b'}$,

(20) Glendening, E. D.; Reed, A. E.; Carpenter, J. E.; Weinhold, F. *NBO*, version 3.1.

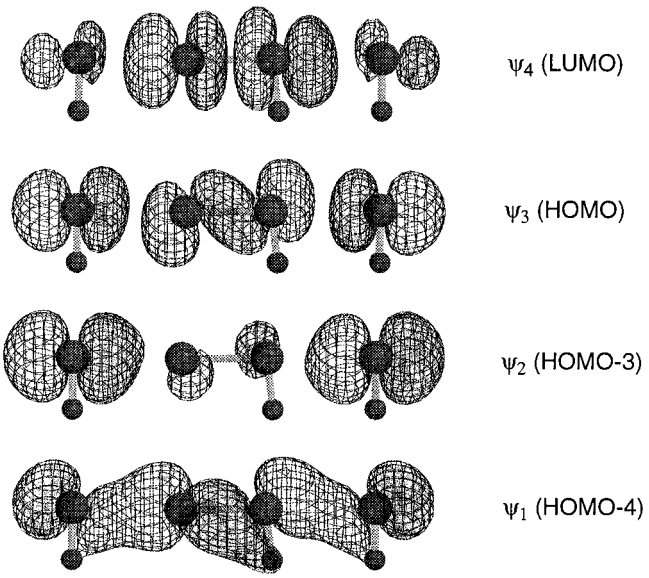


**Figure 3.** The 4c-6e model for the four linear Se atoms with molecular orbitals being drawn for **11a** (see Table 5).

respectively, in model **b**. $\angle^2Se^1SeH_b$ and $\angle^1Se^2SeH_{b'}$ are shown by $\theta_1$ and $\theta_2$, respectively. $r(^1Se-^2Se)$ was fixed at the averaged value of the two structures observed in **2** (3.070 Å). $\angle^1Se^2SeH_{a'}$, $\angle^2Se^1SeH_a$, and the torsional angle of $H_a{}^1Se^2SeH_{a'}$ were fixed at 90.00°, 90.00°, and 0.00°, respectively. The angles, $\angle^2Se^1SeH_b$ ($\theta_1$), $\angle^1Se^2SeH_{b'}$ ($\theta_2$), $\angle H_a{}^1SeH_b$, and $\angle H_{a'}{}^2SeH_{b'}$, and the $r$(Se−H) values were optimized.

The results of the calculations are collected in Table 6. There were two energy minima for $\theta_1$ (=$\theta_2$) = 72.72° (**12a**) and $\theta_1$ (=$\theta_2$) = 157.43° (**12b**) if the calculations were

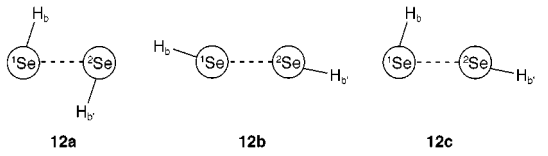


performed with the 6-311++G(3df,2pd) basis sets at the MP2 level. The structure **12c**, for which $\theta_1$ and $\theta_2$ are close to 72° and 157°, respectively, might also be an energy minimum, since the adduct is expected to be the type I and type II pairing proposed by Parthasarathy and co-workers,[12] which could be stabilized by the electron donor−acceptor interaction. However, the optimized structure was **12b** when the calculations were started from $\theta_1$ =72.7° and $\theta_2$ = 157.4° at the MP2 level. As shown in Table 6, calculations at the HF level gave essentially the same results. Natural charges of the H and Se atoms in **12a** and **12b** were also calculated with the natural population analysis,[20] which are also shown in Table 6.

Molecular orbitals were drawn using the MacSpartan program[21] with 3-21G(*) basis sets employing the structures calculated with the 6-311++G(3df,2pd) basis sets at the MP2 level in Table 5 (**11a** and **11b′**). Figures 3 and 4 depict the molecular orbitals of **11a** and **11b′**, respectively. The molecular orbitals of **11b** were essentially the same as those of **11b′**, although not shown. Figure 5 shows the energy diagram in the formation of

(21) Hehre, H. J. *MacSpartan Plus*, version 1.0; Wavefunction Inc.

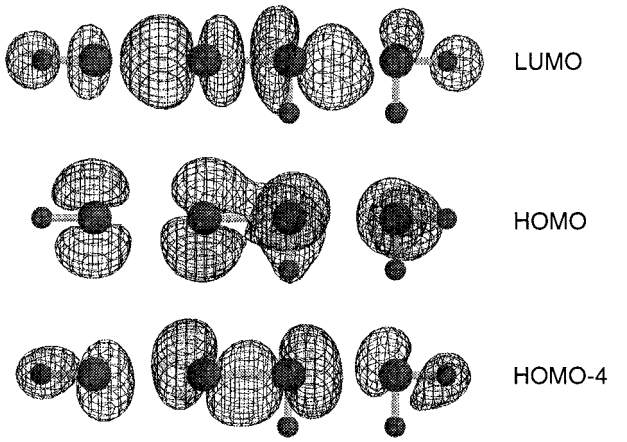


**Figure 4.** Molecular orbitals of linear H−Se···Se−Se···Se−H bond in **11b′**.

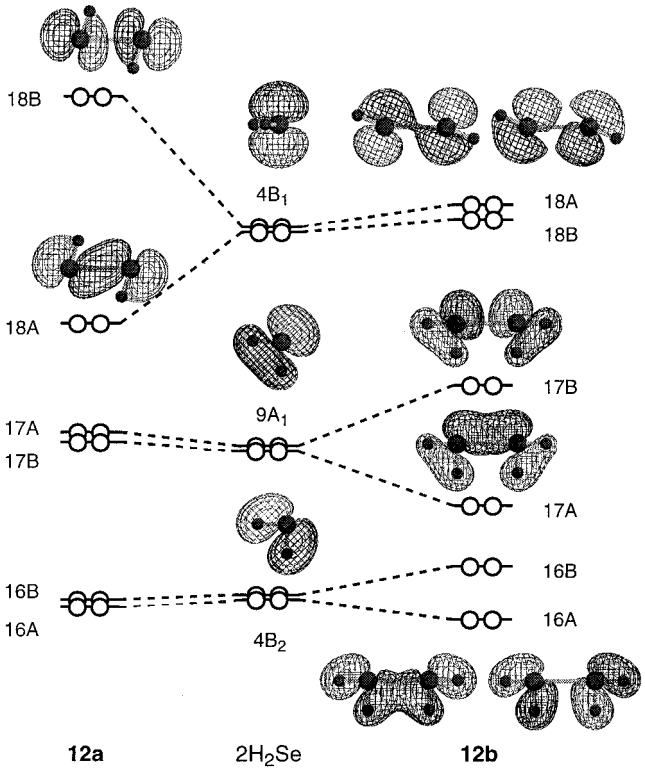


**Figure 5.** Energy diagram for the formation of **12a** and **12b** from $2H_2Se$, together with some molecular orbitals of the species.

**12a** and **12b** from $2H_2Se$, which also contains some molecular orbitals drawn using the program with 3-21G(*) basis sets for the structures calculated with the 6-311++G(3df,2pd) basis sets at the MP2 level shown in Table 6. Table 7 shows the energies of some orbitals for **12a**, **12b**, and $H_2Se$ calculated with the 6-311++G-(3df,2pd) basis sets at the MP2 level.

Before discussion of the nature of the 4c-6e bond in **1**, we would like to discuss the case of **2** first. As shown in Table 6, two structures, **12a** and **12b**, were found to be the energy minima. The structure **12b** was more stable than **12a** by 0.0198 au (52.0 kJ $mol^{-1}$), and the former

(22) The calculations exhibit that the adduct will form two $H_2Se$ molecules if there is no framework to join the two selenide molecules (or groups) such as in the naphthylidene group.

**Table 7. Energies and Characters of Molecular Orbitals of $H_2Se$, 12a, and 12b Calculated with the 6-311++G(3df,2pd) Basis Sets at the MP2 Level[a]**

| $H_2Se$ | 12a | 12b |
|---|---|---|
| −9.80 (4B1) | −8.00 (18B) | −9.57 (18A) |
| | −11.17 (18A) | −9.85 (18B) |
| | (−9.58 (av)) | (−9.71 (av)) |
| −13.03 (9A1) | −12.79 (17A) | −12.11 (17B) |
| | −12.95 (17B) | −13.92 (17A) |
| | (−12.87 (av)) | (−13.01 (av)) |
| −15.13 (4B2) | −15.13 (16B) | −14.85 (16B) |
| | −15.16 (16A) | −15.55 (16A) |
| | (−15.15 (av)) | (−15.20 (av)) |

[a] In electronvolts.

was less stable than two $H_2Se$ molecules by 0.0056 au (14.7 kJ $mol^{-1}$) at the MP2 level.[22] The natural charges at the Se, $H_a$, and $H_b$ atoms ($Q_n$(Se), $Q_n(H_a)$, and $Q_n(H_b)$, respectively) in **12a** became more positive, negative, and negative by 0.0060, 0.0044, and 0.0016, respectively, relative to those of the corresponding atoms of $H_2Se$ at the MP2 level. On the other hand, the charges at the atoms in **12b** were estimated to be more positive, negative, and negative by 0.0077, 0.0014, and 0.0062, respectively, by similar calculations. These results suggest that the lone pair−lone pair interaction between selenium atoms in the almost linear alignment of $H_b$−Se···Se−$H_b$ in **12b** expels electrons of the Se atoms to the $H_b$ atoms while the $H_a$ atoms accept electrons more effectively in **12a** than in **12b**. The results obtained at the HF level were almost the same as those obtained at the MP2 level.

As shown in Figure 5, the interaction between the p-type lone pairs ($4B_1$ of $H_2Se$) in **12a** forms $\sigma$- and $\sigma$*-type orbitals (18A and 18B, respectively) while that in **12b** gives $\pi$- and $\pi$*-type orbitals (18B and 18A, respectively). The interaction in **12a** is stronger than that in **12b**. The $\pi$-type orbitals extend more effectively on the $H_b$ atoms than the $\sigma$-type orbitals in **12a**. The orbitals extend on the $H_a$ atoms more effectively in **12a** than in **12b**, although not shown. This may be a reason that the $H_a$ atoms in **12a** and the $H_b$ atoms in **12b** accept electrons effectively. On the other hand, the $9A_1$ (the s-type lone pair) and $4B_2$ orbitals of $H_2Se$ interact more effectively in **12b** than in **12a** (17A,B and 16A,B, respectively). Such interactions in **12b** can be characterized by the $\sigma$-type $4p_x$−$4p_x$ orbitals extending over the adduct containing the almost linear $H_b$−Se···Se−$H_b$ framework. Molecular orbitals in **12a** are complex and difficult to understand by a simple image, so they are not depicted except 18A and 18B.

The energy difference between 18A and 18B and the averaged value for the two orbitals is larger in **12a** than in **12b**, as shown in Table 7. The interaction between the two $4B_1$ orbitals of $2H_2Se$ should be larger in the $\sigma$-type overlap in **12a** than in the $\pi$-type overlap in **12b**, resulting in the larger energy difference in the former than in the latter.[23] The larger overlap integral in the $\sigma$-type interaction must cause the larger exchange repulsion[24] in **12a** relative to **12b**, since the two $4B_1$ orbitals are filled with two electrons, which would be the reason the averaged energy of 18A and 18B in **12a** is larger than that in **12b**, and that, in turn, would be the reason **12a** is estimated to be less stable than **12b**. The severe exchange repulsion pointed out in the $\sigma$-type interaction in **12a**[25] must be avoided in the distorted $\pi$-type interaction in **12b**.

If the two orbitals, 18A and 18B, are filled with only three electrons, the total energy of the $\sigma$- and $\sigma$*-orbitals in **12a** would be significantly reduced and they would be more stable than the $\pi$- and $\pi$*-orbitals in **12b**. (The total energies of the two orbitals in **12a** and **12b** would be the same if 0.32 electrons were taken away from the orbitals of the model.) Such orbital interactions are predicted for 4c-6e in **11a**, which will be discussed later. Although the 17A,B and 16A,B in **12b** are constructed based on the typical $\sigma$-type interactions, the orbitals are evaluated to be not so destabilized, since the orbitals extend not only over the two Se atoms but also over the four hydrogens. The contribution of the vacant orbitals to the 17A,B and 16A,B in **12b** should also reduce their energies.

After establishment of the character of the lone pair−lone pair interaction in model **b**, we would like to examine the nature of the chemical bond in model **a**. As shown in Table 5, two energy minima, **11a** and **11b**, were found at the MP2 level.[26] Although **11a** was evaluated to be less stable than **11b** by 0.0013 au (3.4 kJ $mol^{-1}$), the structure **11a** reproduced well the observed X-ray crystallographic results of **1**. The two phenyl groups in **1** must play an important role for **1** to form a 4c-6e structure; the p-type lone pairs of the Se atoms of the phenylselanyl groups can interact with the $\pi$-orbitals of the phenyl group, and the interaction must be highly effective if the phenyl rings in **1** are perpendicular to the linear four Se atoms. The orientation of the phenyl groups in **1** satisfies the requirement of the orbital interaction in model **a**. The phenyl groups may also accept some electrons from the p-type lone pairs of the selenium atoms in **1**. The optimized structure of **11a** depicts that the linear alignment of the four Se atoms in **1** must be due to the energy-lowering effect of the linear alignment rather than the crystal-packing effect in the crystal. The role of the phenyl groups will be examined by the MO calculations on model **c**.

As shown in Table 5, the central Se−Se distance ($r(^2Se,^3Se)$) in **11a** becomes longer relative to that of $Se_2H_2$ by 0.06 Å, which strongly suggests that the charge transfer must take place from the outside Se atoms to the central $\sigma$*(Se−Se) bond. The natural population analysis revealed the character of the charge transfer in the adducts; the $Q_n(^1Se)$ and $Q_n(^2Se)$ values of **11a** become more negative and positive, respectively, relative to those of the $Se_2H_2$ and $SeH_2$ by ca. 0.05. The $Q_n$(H) values of $Se_2H_2$ and $SeH_2$ changed similarly to those of the Se atoms to which hydrogens were joined, although the magnitudes were smaller. These results strongly support the idea that the character of the charge transfer in **11a** is that from the two outside Se atoms (or $SeH_2$ molecules) to the central $\sigma$*(Se−Se) bond (or the central $Se_2H_2$). The bond constructed by the four Se atoms can be well described with the 4c-6e model. The character of the charge transfer in the 4c-6e model in **11a** is very different

(23) Hirschfelder, J. O.; Linnett, J. W. *J. Chem. Phys.* **1950**, *18*, 130. Moore, N. *J. Chem. Phys.* **1960**, *33*, 471.

(24) The energy levels of 18A and 18B are suggested to intersect as the $\theta$ value becomes larger from that in **12a** to that in **12b**.

(25) The results of the calculations explain well the UPS of 1,2-bis(methylthio)naphthalene and naphtho[1,8-*b*,*c*]-1,5-dithiocin,[5b] although the dithiocin is in a cisconformation around the thio groups, while **12a** is in a transconformation.

(26) The results calculated at the HF level are adequately reliable, we believe, since those calculated on model **b** at the HF level are very similar to those at the MP2 level, as shown in Table 6. The fixing of the nonbonded Se−Se distances in model **a** and model **b** must also make the results at the HF level reliable.

**Table 8. Optimized Structures for PhSeH···HSeSeH···HSePh (Model c) and PhSeH···HSeMe (Model d) Calculated with the 6-311+G(d,p) Basis Sets at the B3LYP Level, Together with the Related Compounds**

| | | PhSeH | | | HSeSeH | | MeSeH | | |
|---|---|---|---|---|---|---|---|---|---|
| | E (au) | *r*(Se,C) (Å) | *r*(Se,H) (Å) | ∠CSeH (deg) | *r*(Se,Se) (Å) | *r*(Se,H) (Å) | *r*(Se,C) (Å) | *r*(Se,H) (Å) | ∠CSeH (deg) |
| model **c**[a] | −10072.0134 | 1.9401 | 1.4707 | 90.00[b] | 2.4827 | 1.4733 | | | |
| PhSeH | −2633.8543 | 1.9401 | 1.4707 | 90.00[b] | | | | | |
| HSeSeH[c] | −4804.3167 | | | | 2.3964 | 1.4743 | | | |
| Δ | 0.0123 | 0.0000 | 0.0000 | 0.00 | 0.0863 | −0.0010 | | | |
| model **d**[d] | −5075.9233 | 1.9616 | 1.4749 | 94.43 | | | 1.9889 | 1.4729 | 94.28 |
| PhSeH | −2633.8550 | 1.9508 | 1.4753 | 95.20 | | | | | |
| MeSeH | −2442.0760 | | | | | | 1.9776 | 1.4732 | 95.19 |
| Δ | 0.0077 | 0.0108 | −0.0004 | −0.77 | | | 0.0133 | −0.0003 | −0.91 |

[a] The nonbonded *r*(Se,Se) value was fixed at 3.053 Å. [b] The ∠CSeH value was fixed at 90.00°. [c] The ∠SeSeH value and the torsional angle ∠HSeSeH were fixed at 90.00°. [d] The nonbonded *r*(Se,Se) value was fixed at 3.070 Å, and the $\theta_1$ and $\theta_2$ values in Scheme 2 were optimized to be 153.80° and 153.82°, respectively.

from that of the 3c-4e model.[27] The character in the 3c-4e model is that from the central atom to the outside ligands, which forms a highly polar hypervalent bond.

Character of charge transfer in the 4c-6e: $Z^{\delta+}\cdots Z^{\delta-}-Z^{\delta-}\cdots Z^{\delta+}$.

Character of charge transfer in 3c-4e: $Z^{\delta-}-Z^{\delta+}-Z^{\delta-}$.

The molecular orbitals constructed by the linearly aligned four Se atoms are depicted in Figure 3 exemplified by **11a**. The molecular orbitals are mainly constructed by the $\sigma$-type interactions between two $p_x$ orbitals of the outside Se atoms ($np_x$(Se)) and the $\sigma$(Se−Se) and $\sigma^*$(Se−Se) orbitals of the central Se atoms, yielding four new molecular orbitals, $\psi_1$, $\psi_2$, $\psi_3$, and $\psi_4$. The $\psi_1$ orbital mainly consists of the $\sigma(^1Se-^3Se)$ orbital and the two $np_x$(Se) orbitals without any nodal plane between the Se atoms. The $\psi_2$ orbital extends over the two $np_x$ orbitals of the outside Se atoms with smaller extension over the central Se atoms. The $\psi_3$ orbital, which is the HOMO, also mainly consists of the $\sigma(^1Se-^3Se)$ orbital and the two $np_x$(Se) orbitals with two nodal planes between the Se−Se bonds. The $\psi_4$ orbital (LUMO) has the contribution of the $\sigma^*(^1Se-^3Se)$ orbital with smaller contributions of the two $np_x$(Se) orbitals. These results, containing the fact that the $\psi_3$ and $\psi_4$ are the HOMO and LUMO, respectively, show that the bond should be analyzed by the 4c-6e model.[27]

The calculations on model **a** gave another minima, shown as **11b**. Some molecular orbitals of the linear $H_c-Se\cdots Se-Se\cdots Se-H_c$ bond in **11b′** are shown in Figure 4, which are essentially the same as those of **11b**. The linear molecular orbitals are constructed by the interactions between the central $\sigma$(Se−Se) and $\sigma^*$(Se−Se) orbitals and the $9A_1$ and $4B_2$ orbitals of the outside $H_2Se$ in **11b′**. Indeed, the LUMO and HOMO-4 orbitals extend mainly over the linear $H_c-Se\cdots Se-Se\cdots Se-H_c$ atoms, but other orbitals are contributed by the atomic orbitals perpendicular to the line or on the $H_a$ (and $H_b$) atoms. Therefore, it would not be suitable for the linear $H_c-Se\cdots Se-Se\cdots Se-H_c$ bond to be analyzed by the 6c-6e model based on the MO calculations. The character of charge transfer in the formation of **11b′** is from the outside $H_c$ to the four Se atoms, accompanied by the enlarged *r*(Se−H) and *r*(Se−Se) values, although the magnitudes are small. The character of the charge transfer in the formation of **11b** is similar to that in the case of **11a**, except for $H_c$. The interpretation based on the 4c-6e model may also be valid for the four Se atoms even in **11b**.

**Scheme 2**

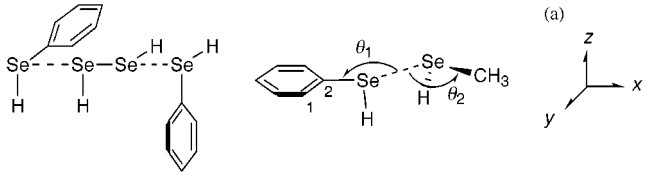


model **c** model **d**

The effects of the $\pi$-orbitals of the phenyl groups on the 4c-6e bond in **1** and the 2c-4e bond in **2** were also examined. Ab initio MO calculations were performed on the adducts, PhSeH···HSeSeH···HSePh (model **c**) and PhSeH···HSeMe (model **d**), where naphthylidene groups in **1** and **2** were replaced by hydrogens, with the 6-311+G(d,p) basis sets at the DFT (B3LYP) level. Scheme 2 shows the structures of model **c** and model **d**, together with the axes (cf. Scheme 2a). The four Se atoms in model **c** were placed on the *x*-axis, its six Se−X (X = H and C) bonds were in the *y*- or *z*-direction, and the two phenyl planes were on the *yz*-plane. The nonbonded *r*(Se,Se) values were fixed at 3.053 Å. Meanwhile, benzeneselenol was also calculated as the planar structure by the same method with the CSeH angle being fixed at 90.00°. The structure of the phenyl group was employed in the calculations of model **c** without further optimization. The six Se−X and the central Se−Se bond distances were optimized. While the *r*(Se,Se) value of the HSeSeH moiety in model **c** became larger than that of free HSeSeH, the *r*(Se,C) and *r*(Se,H) values of the PhSeH groups were coincidentally the same for both the adduct and the free compound. The C(1), C(2), Se(Ph), Se(Me), and C(Me) atoms in model **d** were placed on the *xy*-plane with the Se···Se distance being fixed at 3.070 Å. The torsional angle between the Se−H and C(1)−C(2) bonds in PhSeH was assumed to be 90.00°. Other values containing the torsional angles in the phenyl plane were optimized. The $\theta_1$ and $\theta_2$ values in model **d** were optimized to be 153.80° and 153.82°, respectively, and the *r*(Se,C) values became larger relative to those of the free components. The slight deviation from the *xy*-plane was also observed for the phenyl group. The results are summarized in Table 8.

(27) (a) Pimentel, G. C. *J. Chem. Phys.* **1951**, *19*, 446. Musher, J. I. *Angew. Chem., Int. Ed. Engl.* **1969**, *8*, 54. (b) Chen, M. M. L.; Hoffmann, R. *J. Am. Chem. Soc.* **1976**, *98*, 1647. (c) Cahill, P. A.; Dykstra, C. E.; Martin, J. C. *J. Am. Chem. Soc.* **1985**, *107*, 6359. See also: Hayes, R. A.; Martin, J. C. Sulfurane Chemistry. In *Organic Sulfur Chemistry: Theoretical and Experimental Advances*; Elsevier Scientific: Amsterdam, 1985.

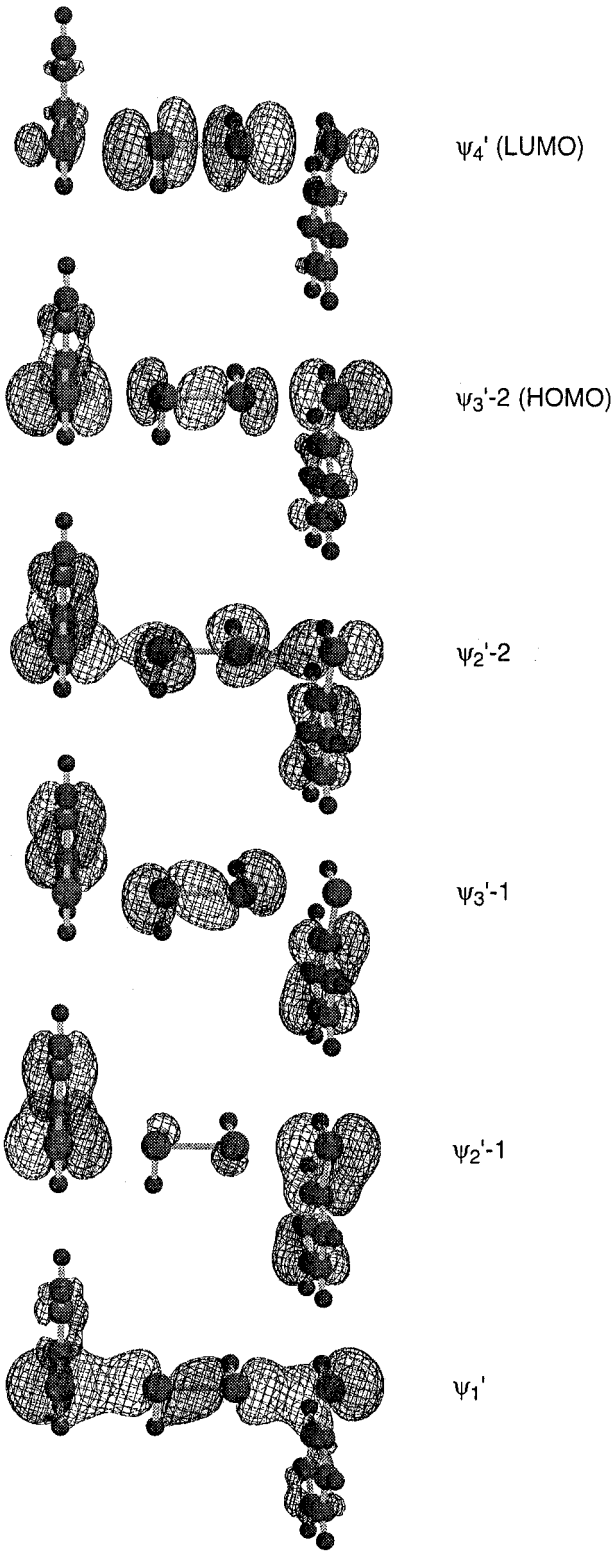


**Figure 6.** Some molecular orbitals in model **c**.

The new molecular orbitals produced by the interaction between the 4c-6e orbitals ($\psi_i$) and the $\pi$-orbitals of the phenyl groups in **1** are shown by $\psi_i'$, named after $\psi_i$. The $\pi$-orbitals interact effectively with $\psi_2$ and $\psi_3$; they hardly interact with $\psi_4$ and interact a little with $\psi_1$, which also interacts with the Se−C $\sigma$-orbitals. Figure 6 shows $\psi_1'$, $\psi_2'$, $\psi_3'$, and $\psi_4'$ for model **c**. Figure 7 shows the HOMO and HOMO-1 for model **d**. The $\pi$-orbitals do not interact with the 2c-4e orbitals due to the orthogonality of the two systems. The p-type lone-pair orbitals in model **d** are estimated to interact only weakly with each other, which may be due to the energy difference caused by the methyl and phenyl groups compared with that of $H_2Se$. (The energies of p-type lone pairs in HSeH, MeSeH, and PhSeH are evaluated to be −0.2523, −0.2309, and −0.2391 au, respectively, with the 6-311+G(d,p) basis sets at the B3LYP level.) The structure of model **d** demonstrates that the type C structure of **2** must come from the 2c-4e interaction in the bis-selenide. The 2c-4e orbitals in **2** are thought again to interact more easily with the naphthyl $\pi$-system than with the phenyl $\pi$-system.

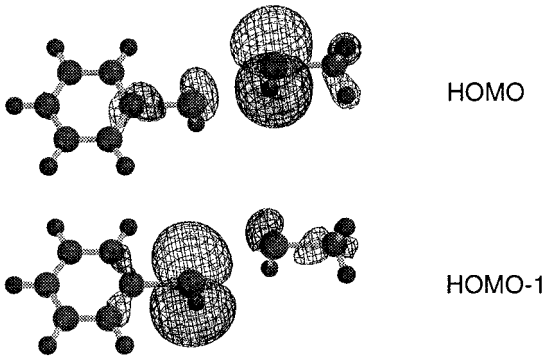


**Figure 7.** HOMO and HOMO-1 in model **d**.

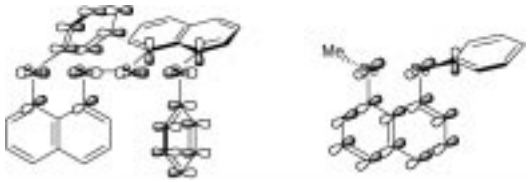

Alvarez et al. discussed the interaction of two bromine molecules to form a $Br_2$ dimer, which reacts with strong electron donors such as alkali metals to form the $Br_4^{2-}$ adduct.[28] If the four Br atoms in the $Br_2$ dimer align linearly, the linear bond can be analyzed by the 4c-4e model, where the four Br atoms interact as Br−Br···Br−Br. On the other hand, for the four Br atoms in the $Br_4^{2-}$ adduct, the linear bond constructed by the four Br atoms can be analyzed with the 4c-6e model, for which interaction must be $[Br\cdots Br-Br\cdots Br]^{2-}$. The bonding scheme of the 4c-6e model in the $Br_4^{2-}$ adduct is very similar to that constructed by the linear four Se atoms discussed above. The bonding scheme in $I_4^{2-}$ ion must also be analyzed by the 4c-6e model.[29] Furukawa and co-workers reported the structure of 1,5-dithioniabicyclo[3.3.0]octane bis(trifluoromethanesulfonate).[3b] In this structure, the two gegen anions located on the direction of the $S^+-S^+$ bond to form a linear $CF_3SO_3^-\cdots S^+-S^+\cdots{}^-O_3SCF_3$ bond. The linear alignment of the $XO^-\cdots S^+-S^+\cdots O^-X$ bond shows that there are two energy minima for the two anionic species in the direction of the dicationic S−S bond, which may also be explained by the 4c-6e model. The X−Z−Z−X bonds constructed with chalcogens and halogens such as the I−Te−Te−I[30] bond might also be

(28) Alvarez, S.; Mota, F.; Novoa, J. *J. Am. Chem. Soc.* **1987**, *109*, 6586.
(29) Siepmann, R.; von Schnering, H. G. *Z. Anorg. Allg. Chem.* **1968**, *357*, 289.
(30) Fujihara, H.; Uehara, T.; Erata, T.; Furukawa, N. *Chem. Lett.* **1993**, 263.

analyzed by the model if the bonds are linear. The linear bonds constructed by more than four atoms[31−33] and macrocyclic frameworks[34] are also reported.

Novel properties caused by the linear 4c-6e bond have been of interest. Such properties were looked for, and we have examined the susceptibility of the substituent effect on $^{77}$Se NMR chemical shifts of the atoms constructing the bond. Ab initio MO calculations containing nonbonded interactions are also in progress. The results will be presented elsewhere.

## Experimental Section

Chemicals were used without further purification unless otherwise noted. Solvents were purified by standard methods. Melting points were uncorrected. $^1$H, $^{13}$C, and $^{77}$Se NMR spectra were measured at 400, 100, and 76 MHz, respectively. The $^1$H, $^{13}$C, and $^{77}$Se chemical shifts are given in ppm relative to those of internal $CHCl_3$ slightly contaminated in the solution, $CDCl_3$ as the solvent, and external MeSeMe, in the three types of spectroscopy respectively. Column chromatography was performed on silica gel (Fujidebison BW-300) and acidic alumina (E. Merk).

**Bis[8-(phenylselanyl)naphthyl]-1,1′-diselenide (1).** To a solution of the dianion of naphtho[1,8-*c*,*d*]-1,2-diselenol, which was prepared by reduction of the diselenol with $NaBH_4$ in an aqueous THF solution, was added benzenediazonium chloride at low temperature. After a usual workup, the solution was chromatographed on silica gel containing acidic alumina. Recrystallization of the chromatographed product from hexane gave **1** as a yellow solid in 66% yield, mp 161−163 °C: $^1$H NMR ($CDCl_3$, 400 MHz) 7.10−7.20 (m, 8H), 7.20−7.27 (m, 4H), 7.35 (t, 2H, $J$ = 7.6 Hz), 7.66 (br d, 2H, $J$ = 7.8 Hz), 7.85 (br d, 2H, $J$ = 7.3 Hz), 7.96 (dd, 2H, $J$ = 7.4 and 1.0 Hz), 8.08 (br d, 2H, $J$ = 6.8 Hz); $^{13}$C NMR ($CDCl_3$, 100 MHz) 125.87, 126.66, 126.69, 127.55, 128.17, 129.26, 130.31, 130.38, 130.99, 132.24, 135.54, 135.74, 136.25, 138.98; $^{77}$Se NMR ($CDCl_3$, 76 MHz) 429.0, 534.2 ($^4J$(Se,Se) = 341.4 Hz). Anal. Calcd for $C_{32}H_{22}Se_4$: C, 53.21; H, 3.07. Found: C, 53.12; H, 3.09.

**1-(Methylselanyl)-8-(phenylselanyl)naphthalene (2).** The diselenide **1** was reduced by $NaBH_4$ in an aqueous THF solution then allowed to react with methyl iodide giving **2** (Y= H) as a white solid in 87% yield, mp 101.5−102.5 °C: $^1$H NMR ($CDCl_3$, 400 MHz) $\delta$ 2.34 (s, 3H, $J$ (Se,H) = 14.1 Hz), 7.19−7.25 (m, 4H), 7.34 (t, 1H, $J$ = 7.8 Hz), 7.37−7.42 (m, 2H), 7.63 (dd, 1H, $J$ = 7.3 and 1.4 Hz), 7.70 (dd, 1H, $J$ = 8.0 and 1.0 Hz), 7.71 (dd, 1H, $J$ = 8.0 and 1.1 Hz), 7.73 (dd, 1H, $J$ = 6.8 and 1.2 Hz); $^{13}$C NMR ($CDCl_3$, 100 MHz) 13.38 ($J$ = 72.8 and 16.6 Hz), 125.86, 125.92, 127.29, 128.30, 129.22, 129.32, 131.21, 131.94, 132.37, 133.13 ($J$ = 11.5 Hz), 135.29, 135.31, 135.54, 135.80; $^{77}$Se NMR ($CDCl_3$, 76 MHz) 434.3, 235.4 ($^4J$(Se,Se) = 322.4 Hz). Anal. Calcd for $C_{17}H_{14}Se_2$: C, 54.27; H, 3.75. Found: C, 54.33; H, 3.73.

**X-ray Structural Determination.** X-ray diffraction data were collected on a Rigaku AFC7R four circle diffractometer with graphic monochromated Cu Kα radiation ($\lambda$ = 1.541 78 Å) and a Mac Science MXC18 machine with graphic monochromated Mo Kα radiation ($\lambda$ = 0.710 69 Å) for **1** and **2**, respectively. The scan type was the $\omega-2\theta$ method. The structure was solved by direct methods (SHELXS86[35]) and refined by the full-matrix least-squares method using the teXsan[36] program. Anisotropic thermal parameters were employed for non-hydrogen atoms, and isotropic parameters were used for hydrogens. The positional and thermal parameters of some hydrogen atoms in the Fourier map in **2** were fixed during the refinement. The function minimized was $\Sigma[\omega(|F_o| - |F_c|)^2]$, where $\omega = (\sigma_c^2|F_o|)^{-1}$. Additional crystal and analysis data are listed in Table 1.

**MO Calculations.** Ab initio molecular orbital calculations were performed on a Power Challenge L computer using the Gaussian 94 program with the 6-311++G(3df,2pd) basis sets at the HF and MP2 levels. The 6-311+G(d,p) basis sets at the DFT (B3LYP) level were also employed for the calculations of models containing the phenyl group(s) and the related compounds. The molecular orbitals in Figures 3−7 were drawn by a Power Macintosh 8500/180 personal computer using the MacSpartan Plus program (version 1.0) with 3-21G(*) basis sets.

**Acknowledgment.** This paper is dedicated to Professor Michinori Ōki on the occasion of his 70th birthday. This work was partly supported by a Grant-in-Aid for Scientific Research (no. 09640635) (W.N.) and that on Priority Areas (no. 09239232) (W.N.) from the Ministry of Education, Science, Sports and Culture, Japan.

**Supporting Information Available:** X-ray structural information on **1** and **2** (56 pages). This material is contained in libraries on microfiche, immediately follows this article in the microfilm version of the journal, and can be ordered from the ACS; see any current masthead page for ordering information.

JO980885L

(31) Dixon, D. A.; Arduengo, A. J., III. *Inorg. Chem.* **1990**, *29*, 970.
(32) Havinga, E. E.; Boswijk, K. H.; Wiebenga, E. H. *Acta Crystallogr.* **1954**, *7*, 487. Dubler, E.; Linowsky, L. *Helv. Chim. Acta* **1975**, *58*, 2604. Millan, A.; Bailey, P. M.; Maitlis, P. M. *Chem. Soc., Dalton Trans.* **1982**, 73. Buse, K. D.; Keller, H. J.; Pritzkow, H. *Inorg. Chem.* **1977**, *16*, 1072.
(33) Bock, H.; Havlas, Z.; Rauschenbach, A.; Nather, C.; Kleine, M. *Chem. Commun.* **1966**, 1529.
(34) Blake, A. J.; Lippolis, V.; Parsons, S.; Schröder, M. *Chem. Commun.* **1996**, 2207.
(35) Sheldrick, G. M. In *Crystallographic Computing, 3*; Sheldrick, G. M., Kruger, C., Doddard, R., Eds.; Oxford University Press: Oxford, England, 1985; p 175.
(36) *TEXSAN: Single-crystal Structure Analysis Software*, version 5.0; Molecular Structure Corp.: The Woodlands, TX, 1981.